Puzzling out the ecological niche construction for nitrogen fixers in a coastal upwelling system

Marcos Fontela[1], Daniel Fernández Román[2], Esperanza Broullón[3], Hanna Farnelid[4], Ana Fernández-Carrera[5], Emilio Marañón[2], Sandra Martínez-García[2], Tamara Rodríguez-Ramos[6], Marta M. Varela[6], Beatriz Mouriño-Carballido[2]

Corresponding author: mfontela@iim.csic.es

Marcos Fontela, Instituto de Investigacións Mariñas (IIM-CSIC), Eduardo Cabello 6 - CP 36208 Vigo, Pontevedra, Spain

[1]Instituto de Investigacións Mariñas (IIM-CSIC), Vigo, Spain

[2]Centro de Investigación Mariña da Universidade de Vigo (CIM-UVIGO), Vigo, Spain

[3]Ocean and Earth Science, National Oceanography Centre, University of Southampton, Southampton, UK

[4]Department of Biology and Environmental Science, Centre for Ecology and Evolution in Microbial Model Systems (EEMiS), Linnaeus University, Kalmar, Sweden

[5] Instituto de Oceanografía y Cambio Global, Universidad de Las Palmas de Gran Canaria (ULPGC), 35214, Las Palmas, Spain.

[6]Centro Nacional Instituto Español de Oceanografía, (IEO-CSIC), Centro Oceanográfico de A Coruña, Paseo Marítimo Alcalde Francisco Vázquez, nº 10, 15001, A Coruña, Spain.

Running title: Diazotrophs niche in upwelling bays

Abstract

Diazotrophs are a diverse group of microorganisms that can fertilize the ocean through biological nitrogen fixation (BNF). Due to the high energetic cost of this process, diazotrophy in nitrogen-replete regions remains enigmatic. We use multidisciplinary observations to propose a novel framework for the ecological niche construction of nitrogen fixers in the upwelling region off NW Iberia — one of the most productive coastal regions in Europe — characterized by weak, and intermittent wind-driven upwelling and the presence of bays. The main diazotroph detected (UCYN-A2) was more abundant and active during summer and early autumn, coinciding with relatively high temperatures (>16ºC), low nitrogen:phosphorus ratios (N:P <7.2), and a large contribution of ammonium (>75%) to the total dissolved inorganic nitrogen available. Furthermore, nutrient amendment experiments showed that BNF is detectable when phytoplankton biomass and productivity are nitrogen limited. Seasonally recurrent biogeochemical processes driven by hydrography create an ecological niche for nitrogen fixers in this system. During the spring-summer upwelling, non-diazotroph autotrophs consume nitrate and produce organic matter inside the bays. Thereafter, the combined effect of intense remineralization on the shelf and sustained positive circulation within the bays in late summer-early autumn, conveys enhanced ammonium content and excess phosphate into the warm surface layer. The low N:P ratio confers a competitive advantage to diazotrophs since they are not restricted by nitrogen supply. The new nitrogen supply mediated by BNF could extend the productivity period and may be key reason why upwelling bays are more productive than upwelled offshore waters.

Keywords: biological nitrogen fixation, ecological niche, upwelling bays, NW Iberia upwelling, nitrogen limitation

Introduction

Nitrogen (N) is a key element in the biosphere which limits the growth of primary producers in marine and land ecosystems[1]. Despite being very abundant in the atmosphere, it is only available for a reduced group of organisms, termed diazotrophs, able to reduce atmospheric dinitrogen (N_2) gas into biologically assimilable forms, through biological dinitrogen fixation (BNF). The traditional focus on archetypal marine N_2-fixers (filamentous cyanobacteria and diatom-diazotroph associations) has been expanded to include unicellular cyanobacteria and multiple groups of heterotrophic bacteria and Archaea[2]. While the BNF activity of some of these groups is still uncertain or biogeochemically insignificant[3], the small diazotrophic cyanobacteria *Candidatus* Atelocyanobacterium thalassa (hereafter UCYN-A) has emerged as a key player in the marine nitrogen cycle[4], showing characteristics of a N_2-fixing organelle, or "*nitroplast*"[5].

Despite decades of intense research, the control factors of diazotrophy remain enigmatic. It was traditionally assumed that the ability to access the vast atmospheric N_2 pool gives ecological advantage to diazotrophs where and when fixed N concentrations are low, whereas BNF would be irrelevant at enhanced availability of combined N resources[2]. However, energetically, fixing N_2 is only marginally (~25%) more costly than using nitrate[6], and recent studies have expanded diazotroph global distribution to N-enriched regions[7–10], including subpolar and polar waters[11–14], coastal zones [15–17], upwelling ecosystems [18–20], and even the aphotic ocean[21].

Methodological approaches to investigate the relevance of control factors on diazotrophy include modeling studies[22, 23], nutrient addition experiments in the lab or with natural populations [6, 24, 25], and database analyses to explore relationships between environmental variables and the presence or activity of diazotrophs[10]. However, deciphering the independent effect of environmental properties on the distribution and

activity of diazotrophs is not trivial. First, because environmental conditions are correlated to each other, and second because nutrient concentration does not necessarily inform about nutrient availability, since low concentrations can be the result of phytoplankton consumption[26]. Few studies have investigated the drivers of diazotrophy in N-enriched regions, revealing correlations with temperature, chlorophyll-a (*Chla*) and inorganic nutrient content[9, 18, 27]. Whether these relationships are circumstantial or the result of control mechanisms for diazotrophy, remains enigmatic.

The coastal upwelling region off the western Iberian Peninsula marks the northern limit of the Canary Current Upwelling Ecosystem, characterized by coastal embayments known as Rías[28]. In this area, upwelling is weak and intermittent, and the Rías are considered an extension of the shelf[29]. The predominance of along-shore northeasterly winds in spring/summer causes seasonal upwelling and positive circulation— surface waters from the Rías moves towards the ocean, while deeper, nutrient-rich oceanic waters flow into the Rías [30, 31]. These nutrient inputs, enhanced by remineralization within the Rías and on the shelf[32], drive, among other factors, high phytoplankton production, which supports one of the most important blue economies based on living resources in Europe [33]. During early spring, when nutrient availability is high, the phytoplanktonic community is dominated by large diatoms and autototrophic nanoflagellates[34], while smaller diatoms and heterotrophs coexist during summer, as regenerated nutrients become more significant [35]. From October to March, prevailing southerly winds promote downwelling events[30, 31] and negative circulation — where surface waters flow into the Rías while deeper waters are expelled - associated with low phytoplankton growth conditions[36].

Knowledge about diazotrophy in this region is limited to a few observations. Relatively low BNF rates, mainly attributed to UCYN-A, were reported in the shelf off Ría de Vigo in summer of 2009[37, 38]. Ten samplings carried out between February 2014 - December

2015 at the shelf off Ría de A Coruña confirmed relatively low BNF rates in the region, which were higher (up to 0.095 nmol N $L^{-1}d^{-1}$) in surface waters during summer upwelling and relaxation[20]. Under these conditions the diazotroph community was dominated by UCYN-A2, whereas with downwelling non-cyanobacterial diazotrophs (i.e. heterotrophic Bacteria and Archaea, hereafter NCD) were dominant[19]. Despite these insights, the factors driving BNF in this system remain unknown, as the limited temporal resolution of previous studies does not allow to reconstruct the environmental conditions accompanying the variability in diazotrophic composition and activity. Here, using a large data set of multidisciplinary observations, we describe in detail the ecological niche construction of nitrogen fixers in the upwelling region off NW Iberia.

Materials and methods

Sampling and hydrography

The dataset comprises 79 one-day sampling events within a period of ~4.5 years (2014-2018, Table S1). All samples belong to four different locations (Fig. S1). There were 10 samplings from the northern limit of the upwelling system, taken in the adjacent shelf off Ría de A Coruña (43.42º N, 8.44º W, 80 m depth) between February 2014 and December 2015 (NICANOR[20]). Next, there were 55 samplings with almost weekly resolution at a central station in the inner Ría de Vigo (42.24º N 8.78º W, 40 m depth) between March 2017 and April 2018 (REMEDIOS-seasonal[39]). Finally, there were 14 samplings along two weeks of summer 2018 with daily resolution (REMEDIOS-cruise[40]). Among them, 10 samples were taken inside the Ría de Pontevedra (42.36ºN 8.78ºW, 30 m depth) and 4 from the outer shelf (42.30ºN 9ºW, ~19.6 km apart, 100 m depth). During each sampling profiles of temperature, salinity and fluorescence were acquired with a SBE25plus CTD (SeaBird Electronics). Surface samples (1-3 m) were collected to determine dissolved inorganic nutrients

(ammonium NH_4^+, nitrite NO_2^-, nitrate NO_3^-, phosphate PO_4^{3-}), chlorophyll *a* (*Chla*), primary production (PP), BNF and DNA and RNA samples.

Samples for the determination of dissolved inorganic nutrients and total *Chla* were collected and frozen at −20ºC [41, 42]. The fluorescence emitted by the *Chla* was measured from pigments extracted in 90% acetone at 4ºC overnight using the spectrofluorometric method[20], and a Turner designs Trilogy fluorometer [43]. Seawater samples were spiked with 2–10 µCi of $NaH^{14}CO_3$ and incubated during 2-3 h starting at noon (REMEDIOS and nutrient addition experiments) or 24 h (NICANOR) in refrigerated incubators simulating the corresponding *in situ* irradiance. More detailed methodological procedures along with comprehensive hydrographic descriptions for each of the sites and conditions can be found in[20, 39, 40]. Since biological samples were restricted to the surface, the environmental parameters included as factors in subsequent statistical analysis are the median value of the first 5 meters of the water column. Inorganic nutrient information has also been interpreted in terms of the N:P ratio, the relationship between total dissolved inorganic nitrogen (DIN) and phosphate:

$$\text{N:P ratio} = DIN / PO_4^{3-} = (NO_3^- + NO_2^- + NH_4^+) / PO_4^{3-}$$

A N:P ratio = 16 denotes the fulfillment of Redfield stoichiometry[44]. Deviations from this ratio provide insights into the nutrient availability: N:P>16 denotes excess nitrogen over phosphorus availability, whereas N:P<16 indicates potential nitrogen limitation and excess phosphate. The fraction of NH_4^+ in total dissolved inorganic nitrogen DIN [$\%NH_4^+ = NH_4^+ / (NO_3^- + NO_2^- + NH_4^+)$], expressed as percentage, was the variable informing about nitrogen speciation.

Biological nitrogen fixation rates

Estimates of BNF activity at surface (1-2 m) are available for 34 sampling dates (43% of total samplings). BNF rates were determined with the $^{15}N_2$ bubble addition technique[45].

Triplicate 2-L acid-cleaned polycarbonate bottles (Nalgene) were sealed with silicone septa caps and 3 mL of $^{15}N_2$ (98 atom%, Cambridge Isotope Laboratories, Lot #I-16727 and #I-19168) were injected with a gas-tight syringe. The bottles were gently mixed, and incubated for 24 hours simulating in situ conditions of temperature and light with running-surface water and neutral-mesh shading to mimic surface irradiance. After incubation, each sample was filtered through pre-combusted (4h, 450°C) 25 mm Whatman GF/F filters, (0.7 µm nominal pore size) using low vacuum (<100mmHg), and filters were stored frozen (−20°C). A time-zero bottle was also filtered to calculate the initial natural abundance of N isotopes in the particulate material. Before analysis, filters were thawed, dried (60°C, 24-48 h) and pelletized in tin capsules. Particulate organic nitrogen and carbon (PON and POC) content, as well as the relative abundance of stable nitrogen isotopes ($^{15}N/^{14}N$) were determined with a continuous-flow isotope-ratio mass spectrometer MAT253 (Thermo Finnigan) coupled to an elemental analyzer EA1108 (Carlo Erba Instruments) through a Conflo III interface (Thermo Finnigan). During analysis, a set of international reference materials were analyzed for δ15N calibration (USGS 40, USGS41a USGS-25, IAEA-N-1, and IAEA-N-2). An analytical measurement error of ± 0.15‰ was calculated for δ15 N; the error estimate was obtained from replicate assays of the laboratory standard acetanilide interspersed between sample analysis. Detection limits and error propagation were evaluated (Table S2) [46] and detection range spans from 0.04 to 0.26 nmol·$L^{-1}d^{-1}$ with a mean of 0.10±0.05 nmol·$L^{-1}d^{-1}$. BNF rates reported for this upwelling ecosystem are likely underestimated due methodological issues[47] and should be viewed as conservative.

Nutrient addition experiments with natural planktonic communities

Four nutrient addition experiments were performed (coinciding with different climatological seasons of 2017) along with the *in situ* sampling of natural planktonic communities at the inner part of Ría de Vigo (Fig. S1). Experimental design was performed in triplicates (3 Whirl-

pak® bags filled with 5.4 L of sample per treatment) and included a control (no additions performed) and two addition treatments: i) NO_3^- treatment, amended with 10-15 μM NO_3^- and ii) NH_4^+ treatment, amended with 10-15 μM NH_4^+. Besides, both addition treatments included a mix of organic nutrients (5 μM glucose and 5 μM amino acids) in all experiments and 1 μM of phosphate (PO_4^{3-}) in winter and spring experiments. A detailed description of the experimental setup is available in Text S1. Experiments lasted 3 days and samples were taken every 24 h to monitor changes in *Chla* and PP. Samples for RNA and BNF rates were collected after 24 h incubation. The magnitude of the responses was estimated as response ratios (RR) between the value of the variable at 24 h in the amendment treatment (AT) and the control (C), AT/C.

Bulk DNA sampling, extraction, nested-amplification of the *nifH* gene and Illumina sequencing

For 71 sampling dates (90% of total) surface water was sampled for DNA collection. Between 7.5 and 10 L of seawater per replicate (4 replicates) were collected and filtered using silicone tubes and peristaltic pumps through sterile STERIVEX 0.22 μm pore size filters (Millipore, USA). Summer samples of July 2018 were prefiltered with a 200 μm mesh filter. Filters were preserved with 1.8 mL of lysis buffer (50 mM Tris-HCl pH 8.3, 40 mM EDTA pH 8.0, 0.75 M sucrose), immersed in liquid nitrogen and subsequently stored at −80 °C until further analysis. DNA was extracted using the PowerWater® DNA Isolation Kit (Mobio, Carlsbad, CA, USA.), quantified and quality-checked (according to the A260/A280 ratio) using a spectrophotometer NanoDrop 2000TM (Thermo Fisher Scientific). Amplification of *nifH* gene and sequencing of the amplicons were performed following [48, 49]. The PCR reactions were run on a T100TM Thermal cycler (BIO-RAD)[19]. The amplified products were purified using PCR Extract Mini Kit (5PRIME) and quantified using a spectrophotometer NanoDrop 2000™ (Thermo Fisher Scientific). Prior to sequencing, an additional PCR amplification of 10 cycles with custom barcoded *nifH1* and *nifH2* primers

was carried out. After purification and library preparation from the barcoded PCR products, paired-end sequencing was performed using the MiSeq® reagent kit with V2 chemistry (500 cycles) at the facilities of IMGM Laboratories GmbH (Germany) on the Illumina MiSeq® Next Generation Sequencing technology (Illumina Inc.).

RNA extraction, cDNA generation and nifH gene quantification

For 15 sampling dates (19% of total) surface water was sampled for RNA collection following the same procedure described for DNA. Total RNA extraction from Sterivex® filters was performed by using 200 µm Low binding Zirconium beads (OPS diagnostics) and QIAGEN RNeasy Mini Kit (Cat.no 74104) and RNase-Free DNase Set (Cat.no 79254). DNase treatment was done with AMBION Turbo DNA free Kit (Invitrogen, Cat.No: AM1907). First-strand cDNA synthesis was done with SuperScript® III First-Strand Synthesis System for RT-PCR, and total RNA concentration was quantified by Nanodrop & Qubit. To quantify *nifH* genes and expression of key diazotrophs identified in the amplicon libraries, 78 and 15 samples were amplified and quantified by quantitative polymerase chain reaction (qPCR) and reverse transcription qPCR (RT-qPCR), respectively, using Taqman primer probe sets (PrimeTime qPCR Assays, Integrated DNA Technologies) (see details in[20]). Briefly, the qPCR assays targeted the *nifH* gene of three common diazotrophic strains, namely UCYN-A2[50], UCYN-A1[51], and γ-Proteobacterium affiliated phylotype γ-24774A11[52] (Table S3). The PrimeTime® Gene Expression Master Mix (IDT), DNA/cDNA template, and primers-probe set (0.5 and 0.25 µM final concentrations, respectively) were combined with PCR grade water (Sigma-Aldrich) to create a final reaction volume of 20 µL. Thermal cycling conditions for the qPCR assay consisted of a 3-minute incubation at 95°C, followed by 45 cycles of 15 seconds at 95°C and 1 minute at 60°C. Each qPCR run included nine 10-fold serial dilutions of standards that contained the targeted *nifH* fragments (gBlocks® Gene Fragments, IDT), and samples were run in triplicate, while standards were run in duplicate. Reactions were performed in a MyiQ2™ Real-Time PCR Detection System (Bio-Rad

Laboratories). Amplification efficiencies were always greater than 90%. We performed inhibition test by several dilutions at certain random samples and we concluded that our samples were not inhibited. The limit of detection (LOD) was 9 *nifH* copies L^{-1}, and the detected but not quantified (DNQ) limit was 87 *nifH* copies L^{-1} for UCYN-A2 and UCYN-A1 and 86 *nifH* copies L^{-1} for Gammaproteobacteria. Abundances below LOD were assigned 0 *nifH* copies L^{-1}, whereas measurements higher than the LOD but less than the DNQ were assigned 1 *nifH* copies L^{-1}.

Bioinformatics and phylogenetic

Paired-end reads were merged, selected and quality filtered, chimera were removed, and Amplicon Sequence Variants (ASVs) were determined with the *dada2* pipeline[53]. Sequences with stop codons or with frameshift errors were excluded from the analysis. Non-*nifH* sequences were filtered out against the database compiled in [54] using the HMMER algorithm. The remaining sequences were aligned to a reference alignment, in the "genome879" *nifH* database (https://wwwzehr.pmc.ucsc.edu/Genome879/). The phylogenetic affiliation of the translated ASVs into the canonical *nifH* clusters defined by [55] was performed by BLASTx[56] using genome-derived sequences from the updated and curated *nifH* database[57] as references. Finally, ASVs were sorted according to their closest affiliation in the BLASTp database (>96% cutoff)[55]. Following BLASTp matching at Genus level, diazotrophs were categorized in 9 taxonomical groups (Class level) for subsequent analytical purposes (Table S4). Rarefaction curves (rarefy function in vegan package[58]) showing a plateauing trend (Fig. S2) confirmed that DNA extraction, sequencing and bioinformatics were appropriately implemented for most samples, and only 4 DNA samples out of 79 were discarded. We established that the diazotrophic community at each individual sample was dominated by Cyanobacteria when UCYN-A relative abundance met two criteria: i) it was the most abundant ASV and ii) it represented

individually more than a third (33%) of total relative abundance. Otherwise, we considered the community dominated by non-cyanobacterial diazotrophs (NCD) (Fig. S3).

Statistical analysis

All statistical analyses were done in R (v4.1.2; R Core Team 2021). The community composition of diazotrophs was investigated by Principal Coordinates Analysis (PCoA, *vegan* package) with an ordination based on Bray-Curtis dissimilarity distances matrix. The environmental parameters were fitted onto the PCoA ordination and represented as vector overlays when their contribution to the observed differences was relevant (*envfit* function in *vegan* package, p-value <0.001).

Then, we assessed the degree of niche overlap among diazotroph taxonomical groups with respect to those relevant environmental drivers identified from the PCoA (sea surface temperature and N:P ratio). Niche overlap analysis is based on nonparametric kernel density estimation[59, 60]. Based on a null model analysis, the difference in niche overlap between groups was considered statistically significant at a p-value<0.01.

Finally, we investigated if those environmental drivers determined ASV's relative abundance. The *corncob* method is based on beta-binomial count regression for correlated observations and is suited for modeling microbial abundances based on high throughput sequencing data[61, 62]. For each individual ASV, a regression model of relative abundance versus environmental data tested the differential abundance across the existent N:P ratio, fraction of NH_4^+ in total DIN and surface water temperature conditions, also controlling the effect of these environmental drivers on the dispersion. A False Discovery Rate of <0.5% was selected as threshold.

Results

Diazotrophic community composition and biological nitrogen fixation

A total of 7030 ASVs were identified based on *nifH* sequencing. The 9 categorized taxonomical groups represented 97.6% of the total ASVs, with *Cyanobacteria* and *Proteobacteria* jointly being 81.6% (45% and 36.6%, respectively) (Fig 1A). The community composition shows similar patterns between sampling sites. The relative abundance of cyanobacterial diazotrophs was large in summer/early autumn while NCD were more relevant in winter/spring, when *Cyanobacteria* were almost absent and the diazotrophic community was more diverse (Fig. S4). UCYN-A2 was the main UCYN-A ecotype and the most abundant ASV. *Deltaproteobacteria* was the second taxa in relative abundance, followed by *Gammaproteobacteria*. The temporal variability of relative abundance based on *nifH* sequencing was coherent with the pattern attained by absolute quantification by qPCR (Fig. 1A, C). Frequently, the quantification of UCYN-A2 was two orders of magnitude larger than UCYN-A1. *Gammaproteobacteria* was below detection limit in more than half of the samples, and their mean absolute abundance was low (708±1600 *nifH* gene copies L^{-1}).

The mean BNF for all samples was 0.92 ± 1.1 nmol N $L^{-1}d^{-1}$ (n = 34), from 0.025 nmol N $L^{-1}d^{-1}$ to 3.17 nmol N $L^{-1}d^{-1}$ (Fig 1B), and it was below detection (i.e., zero) in 11 samples. BNF rates were higher during summer and early autumn in Ría de Vigo and Ría de Pontevedra (2017-2018), whereas they were in general lower in the northernmost location sampled at the shelf off Ría de A Coruña (2014-2015). Higher BNF rates coincided with relatively high *Cyanobacterial* diazotroph gene abundance, whereas NCD dominated the diazotrophic community when BNF rates were undetectable (Fig.1).

The log-transformed abundance of UCYN-A2 *nifH* transcripts (measured by qPCR based on cDNA) exhibited a positive relationship with BNF rates at rates lower than 1.5 nmol N $L^{-1}d^{-1}$ (GAM model, p-value = 0.0617, adjusted R^2 = 0.55, deviance explained = 64%, Fig. 2).

Above this BNF rate, a saturation relationship was observed. Transcription of *nifH* associated to UCYN-A2 also scaled linearly along BNF rates, while no relationship was found between BNF rates and UCYN-A1 *nifH* gene copies or transcripts (Fig. 2).

Environmental control of diazotroph community structure

PCoA analysis confirmed the existence of two groups of samples according to diazotroph community composition (Fig. 3). The first PCoA axis separated samples in which cyanobacterial diazotrophs dominate the community (cyan circles, UCYN-A) from those in which NCD dominated the community (orange squares, NCD). The lower dispersion observed in the UCYN-A group suggests a less diverse phylogenetic community. On the other hand, the larger dispersion of the NCD group[3] suggest higher phylogenetic diversity at the community level. This is confirmed with alpha diversity metrics (Fig. S5). The environmental parameters that most contributed to this community differences are in situ temperature, the fraction of NH_4^+ in total dissolved inorganic nitrogen (%NH_4^+), NO_3^-, N:P ratio and PO_4^{3-} (in that order, complete list of environmental variables and the model fitting coefficients available in Table S5). The N:P ratio, NO_3^- and PO_4^{3-} were negatively associated with temperature and %NH_4^+ in the ordination space. The dominance of UCYN-A in the community was associated with higher temperature and %NH_4^+ concurrent with low N:P ratio.

Kernel density estimates were used to assess the niche overlap of taxonomical groups in terms of temperature, %NH_4^+ in DIN, and N:P ratio (Fig. 4A-C, Table S6). *Cyanobacteria* peaked at 16°C, and they were present at the warmest temperature registered (19-20ºC), whereas NCD groups like *Bacteroidia* and *Proteobacteria* (*Gamma*-, *Epsilon*- and *Betaproteobacteria*) peaked around 13ºC (Fig. 4A). The fraction of ammonium in total dissolved inorganic nitrogen (DIN) was also a differential parameter for cyanobacteria (more present at higher NH_4^+ proportions, >75%) and NCD (which showed higher

abundance at low NH_4^+ proportions, 25%, Fig. 4B). Finally, *Cyanobacteria* occurred preferentially at low N:P ratio conditions (7.2), when there was potential N limitation and excess P, whereas NCD groups have their peak of occurrence at N:P ratios>16 (Fig. 4C).

Additional statistical support at ASV level with beta-binomial count regression models identified 25 ASV differentially-abundant with regard to temperature, 13 ASVs with regard to the fraction of NH_4^+ in DIN, and 10 ASVs that are differentially-abundant across the N:P ratio (out of the 7030 ASV tested, Fig 4D). Only UCYN-A2 has a significant differential abundance related to the three environmental drivers. UCYN-A2 was the only *Cyanobacteria* ASV with a temperature-mediated response, as well as the only ASV with a positive coefficient for the relevance of NH_4^+ in the total DIN, and a negative coefficient for the N:P ratio.

Biological nitrogen fixation is driven by inorganic nitrogen availability

We performed controlled nitrogen amendment experiments to assess whether BNF activity occurs when the phytoplankton standing stock is N-limited, across four seasons (winter, spring, summer and autumn) in the inner Ría de Vigo. As reported previously (Fig. 1), amendment experiments showed higher in situ (natural environment) BNF rates (0.025 nmol N $L^{-1}d^{-1}$ to 3.17 nmol N $L^{-1}d^{-1}$) in summer and autumn, whereas they were below detection limit in winter and spring (Fig. 5A). A significant (ANOVA, p-value <0.05, Fig. 5A) positive response of PP and *Chl a* to nitrogen additions (i.e. phytoplankton standing stock was N-limited) was observed in summer and autumn experiments, coinciding with higher BNF in the field (Fig. 5B). In all seasons with measurable BNF activity, BNF rates were inhibited and significantly reduced when ammonium and nitrate were added, respectively (ANOVA, p-value <0.05, Fig. 5A).

Discussion

UCYN-A2 is the main active N_2-fixer

We revealed through alternative approaches that the abundance of diazotrophs shows seasonality in the NW Iberian upwelling system, with UCYN-A2 being most abundant and active during summer and early autumn. High abundances of *nifH* UCYN-A2 transcripts were concomitant with measurable BNF rates, supporting the link between the expression pattern of UCYN-A2 with BNF rates. This agrees with the current knowledge that UCYN-A2 is more relevant in coastal waters than UCYN-A1[63, 64], and supports the recognition of UCYN-A2 as the main active diazotroph in temperate upwelling regions[65]. UCYN-A2 was also the dominant diazotroph, with comparable BNF rates to those in this study, peaking in summer (ca. 2-3 nmol N $L^{-1}d^{-1}$) in both North Atlantic coastal waters[10] and the Subarctic North Pacific[14]. However, there are at least three lines of evidence that point to an unknown additional group of diazotrophs fixing N in this system. First, the relationship between BNF magnitude and the abundance of UCYN-A reaches a plateau at rates above 1.5 nmol N $L^{-1}d^{-1}$. Second, at the controlled conditions of the experimental nutrient additions, there are no relationship between the change in BNF rates and the absolute abundance of nifH transcript copies L^{-1} quantified by qPCR for UCYN-A2 (Fig. S6). And lastly: when the quantified *nifH* copies L^{-1} are combined with published cell-specific N_2 fixation rates for UCYN-A (~55 fmol N $cell^{-1}$ d^{-1},[66]) and NCD (0.69±1.57 fmol N $cell^{-1}$ d^{-1},[67]), the calculated BNF magnitude is much lower than observed (Fig. S7). The combination of low cell-specific rates and/or low abundance makes the UCYN-A and NCD contribution insufficient to explain the observed BNF rate. Therefore, another key diazotroph player must be involved, being the activity of diatom-diazotroph associations (DDA, [68]) a possible explanation. Diatom-diazotroph associations (DDA) were not detected within our DNA/RNA sequencing. This absence might be surprising, as this coastal upwelling region is dominated by diatoms during the spring-summer productive season [36]. Several diatom genera that are host of

diazotrophs (like *Hemiaulus* or *Rhizosolenia*) are commonly present[69, 70], including in our samples[71]. Although the non-detection of DDA N_2-fixers activity aligns with previous size-fractionated incubations that attributed BNF rates on the shelf off Ría de A Coruña exclusively to small diazotrophs[20], it remains uncertain whether this absence of DDA contribution is due to a methodological bias in the DNA amplification technique[72], or represents a true absence of diazotroph symbionts. To disentangle the contribution of DDA versus UCYN-A in this region, a closer visual inspection of the host cells, a DDA targeted nanoSIMS approach, and/or size-fractionated incubations should be implemented in the future.

Low N content and high temperature are the environmental drivers.

Our results point out to temperature and low nitrogen content (evaluated through the N:P ratio) as the environmental parameters that drive diazotroph community composition and abundance in this coastal upwelling system. The relative enrichment of phosphorus as compared to nitrogen confers a competitive advantage to diazotrophs since they are not restricted by the nitrogen supply. This outcome, confirmed at community, taxa and ASV level, is consistent with previous results. Temperature and N:P ratio have been identified as the main controlling factors of diazotroph abundance in the North Pacific Ocean[27]. Warm temperature (>16ºC) and lower NO_3^- content have been suggested as drivers of UCYN-A2 abundances in the California upwelling region[18]. Additionally, summer observations carried out in the temperate western North Atlantic revealed that diazotroph community composition and BNF correlated positively with *Chla* and P availability[9].

In addition, the short-term increase in PP and *Chla* observed in our nutrient amendment experiments during summer and autumn, when low N:P ratio exists (Fig. 5A), indicates that the phytoplankton standing stock was nitrogen-limited, or at least responsive to nitrogen supply[73]. Interestingly, BNF rates were not completely supressed after NO_3^- addition in the

nutrient amendment experiments. A possible explanation for this is that UCYN-A2 lives in symbiosis with a prymnesiophyte algae (*Braaudosphera bigelowi*) exchanging fixed N for fixed carbon[64, 74]. Indeed, the genome of UCYN-A is so streamlined to fuel BNF that it even lacks genes for carbon fixation, oxygen-evolving photosystem II or nitrate assimilation genes, so it is an obligate N_2-fixer[75, 76], or even a new organelle[5]. Thus, UCYN-A symbiosis relies on N_2 fixation even in N-rich environments[25]. It can be hypothesized that the BNF decreases after nitrogen addition in our microcosms experiments not because of inorganic nutrient inhibition, but due to the eukaryotic host algae being outcompeted by other phytoplankton. Groups such as diatoms, characterized by high maximum nutrient uptake and growth rates[77], may outcompete the slow growing *Braaudosphera*/UCYN-A symbiosis after nutrient additions[78], resulting in decreased BNF.

Puzzling out the diazotrophs niche

Then, how is the diazotroph niche constructed in this coastal upwelling region? We propose a novel framework connecting hydrography and ecology through biogeochemical processes. The full-depth biogeochemical sequence and its connection with surface BNF is shown at a central station at the Ria de Vigo at weekly resolution for the period spring 2017 – spring 2018 (Fig. 6). Starting with hydrography, a key feature of this upwelling system is the bidirectional exchange flow with a two-layer structure[79, 80]. During summer, when upwelling conditions prevail, a positive circulation occurs in the Rías: cold subsurface water enters through the lower layer (Fig. 6A), in contact with the bottom, while warm surface waters flow out toward the shelf[39]. The upwelling causes the uplifting of the relatively young Eastern North Atlantic Central Water (ENACW), which has an N:P ratio above or close to sixteen (Fig. 6B, [29]), and low ammonium content (NH_4^+ <0.5 μmol kg^{-1}, [81]).

Following with ecology, this region shows a rapid phytoplankton response to upwelling pulses[40], as evidenced by the drawdown of inorganic nitrogen and the subsequent

chlorophyll accumulation (Fig. 6 B-D, Fig. S8). After nitrogen drawdown through phytoplankton uptake, a significant fraction of this fresh organic matter is remineralized within 1-2 weeks[81]. This recycling mechanism, also known as nutrient trapping, occurs when particulate organic material sinks out of the photic zone but remains within the upwelling system[81]. The signal of intense bottom remineralization that occurs over the shelf and within the Rías is conveyed into the inner part of the bays, where nutrient trapping processes magnifies, and then uplifts and exits in the surface outflow with the positive circulation[82]. The circulation outflow conveys a remineralization fingerprint that becomes more evident at the surface as the upwelling-favorable season proceeds (Fig. 6B-C). This remineralization fingerprint: (i) decreases the N:P ratio because P remineralization is faster than that of N[83–85], and (ii) accumulates ammonium regenerated within the Ria via ammonification processes[86]. Evidence of cumulative remineralization is reflected in the seasonal evolution of apparent oxygen utilization (AOU), a proxy for the net biological production or consumption of oxygen, calculated as the difference between the observed dissolved oxygen and its saturation concentration (Fig. 7). When AOU at the Ria de Vigo is assessed with discrete samples of measured dissolved oxygen data from 1986-2018[87], it shows lower negative values at the surface during spring and summer due to the oxygen production linked to the synthesis of organic matter by autotrophs. Later, AOU reached its highest positive values in deeper layers as oxygen was consumed during the breakdown of this organic matter (Fig. 7).

We argue that in summer and early autumn, when BNF occurs, the signal from bottom remineralization processes—following the sustained organic matter production during the productive upwelling season—reaches the surface, conveyed by the positive circulation in the Rías (sequential steps schematized in Fig. 8). This creates the optimum niche for BNF in terms of temperature and inorganic nutrient content. The predominance of downwelling

conditions in late autumn/winter, which promote negative circulation in the Rías, combined with low nutrient uptake by phytoplankton due to light limitation[29], and freshwater runoff events reset the inorganic nutrient content in the surface layer to nitrogen replete conditions (Fig. 6)[88], thereby disrupting the diazotroph niche and preventing BNF from occurring. It is uncertain whether only an N:P ratio<16 is important, or the higher contribution of NH_4^+ over NO_3^- to total inorganic nitrogen availability could also be a key factor in the formation of the diazotroph niche. Higher temporal and spatial resolution data covering different environmental conditions and/or multifactorial controlled experiments[89] are needed to unravel the specific role of temperature and the contribution of NH_4^+.

The conceptual framework proposed in our study resembles the mechanistic niche construction previously described in the eastern tropical North Atlantic Ocean [90], where non-diazotrophs facilitate BNF by creating an environment with excess phosphate. However, in our case, the trigger is the combination of predominant positive circulation within the bays during the upwelling season, and the shorter turnover time of phosphorus compared to nitrogen during organic matter remineralization [84]. The specific characteristics of NW Iberia, such us the presence of elongated bays where upwelling is relatively weak and intermittent[29], enable the ecological niche construction for diazotrophy. Despite BNF representing a minor entry of new nitrogen into the euphotic zone compared to other physical processes[20], it may be critical in supporting phytoplankton growth at the end of the productive upwelling season. Therefore, these results could help explain why the upwelling bays are more productive compared to the upwelled offshore waters[32]. Future studies are needed to disentangle what are the key diazotroph players that extend the productive season of the upwelling bays, and the extent to which similar processes occur in other coastal upwelling regions.

Competing Interests statement: The authors declare no competing financial interests

References

1. Gruber N, Galloway JN. An Earth-system perspective of the global nitrogen cycle. *Nature* 2008; **451**: 293–296.
2. Zehr JP, Capone DG. Changing perspectives in marine nitrogen fixation. *Science* 2020; **368**: eaay9514.
3. Turk-Kubo KA, Gradoville MR, Cheung S, Cornejo-Castillo FM, Harding KJ, Morando M, et al. Non-cyanobacterial diazotrophs: global diversity, distribution, ecophysiology, and activity in marine waters. *FEMS Microbiology Reviews* 2023; **47**: fuac046.
4. Martínez-Pérez C, Mohr W, Löscher CR, Dekaezemacker J, Littmann S, Yilmaz P, et al. The small unicellular diazotrophic symbiont, UCYN-A, is a key player in the marine nitrogen cycle. *Nature Microbiology* 2016; **1**: 16163.
5. Coale TH, Loconte V, Turk-Kubo KA, Vanslembrouck B, Mak WKE, Cheung S, et al. Nitrogen-fixing organelle in a marine alga. *Science* 2024; **384**: 217–222.
6. Knapp A. The sensitivity of marine N2 fixation to dissolved inorganic nitrogen. *Frontiers in Microbiology* 2012; **3**.
7. Li D, Jing H, Zhang R, Yang W, Chen M, Wang B, et al. Heterotrophic diazotrophs in a eutrophic temperate bay (Jiaozhou Bay) broadens the domain of N2 fixation in China's coastal waters. *Estuarine, Coastal and Shelf Science* 2020; **242**: 106778.
8. Selden CR, Chappell PD, Clayton S, Macías-Tapia A, Bernhardt PW, Mulholland MR. A coastal N fixation hotspot at the Cape Hatteras front: Elucidating spatial heterogeneity in diazotroph activity via supervised machine learning. *Limnology and Oceanography* 2021; **66**: 1832–1849.
9. Tang W, Wang S, Fonseca-Batista D, Dehairs F, Gifford S, Gonzalez AG, et al. Revisiting the distribution of oceanic N2 fixation and estimating diazotrophic contribution to marine production. *Nature Communications* 2019; **10**: 831.

10. Tang W, Cerdán-García E, Berthelot H, Polyviou D, Wang S, Baylay A, et al. New insights into the distributions of nitrogen fixation and diazotrophs revealed by high-resolution sensing and sampling methods. *The ISME Journal* 2020; **14**: 2514–2526.
11. Harding K, Turk-Kubo KA, Sipler RE, Mills MM, Bronk DA, Zehr JP. Symbiotic unicellular cyanobacteria fix nitrogen in the Arctic Ocean. *Proceedings of the National Academy of Sciences* 2018; **115**: 13371–13375.
12. Raes EJ, van de Kamp J, Bodrossy L, Fong AA, Riekenberg J, Holmes BH, et al. N2 Fixation and New Insights Into Nitrification From the Ice-Edge to the Equator in the South Pacific Ocean. *Frontiers in Marine Science* 2020; **7**.
13. Sato T, Shiozaki T, Taniuchi Y, Kasai H, Takahashi K. Nitrogen Fixation and Diazotroph Community in the Subarctic Sea of Japan and Sea of Okhotsk. *Journal of Geophysical Research: Oceans* 2021; **126**: e2020JC017071.
14. Shiozaki T, Bombar D, Riemann L, Hashihama F, Takeda S, Yamaguchi T, et al. Basin scale variability of active diazotrophs and nitrogen fixation in the North Pacific, from the tropics to the subarctic Bering Sea. *Global Biogeochemical Cycles* 2017; **31**: 996–1009.
15. Bentzon-Tilia M, Traving SJ, Mantikci M, Knudsen-Leerbeck H, Hansen JLS, Markager S, et al. Significant N2 fixation by heterotrophs, photoheterotrophs and heterocystous cyanobacteria in two temperate estuaries. *The ISME Journal* 2015; **9**: 273–285.
16. Hallstrøm S, Benavides M, Salamon ER, Arístegui J, Riemann L. Activity and distribution of diazotrophic communities across the Cape Verde Frontal Zone in the Northeast Atlantic Ocean. *Biogeochemistry* 2022; **160**: 49–67.
17. Mulholland MR, Bernhardt PW, Widner BN, Selden CR, Chappell PD, Clayton S, et al. High Rates of N2 Fixation in Temperate, Western North Atlantic Coastal Waters Expand the Realm of Marine Diazotrophy. *Global Biogeochemical Cycles* 2019; **33**: 826–840.

18. Cabello AM, Turk-Kubo KA, Hayashi K, Jacobs L, Kudela RM, Zehr JP. Unexpected presence of the nitrogen-fixing symbiotic cyanobacterium UCYN-A in Monterey Bay, California. *Journal of Phycology* 2020; **56**: 1521–1533.

19. Moreira-Coello V, Mouriño-Carballido B, Marañón E, Fernández-Carrera A, Bode A, Sintes E, et al. Temporal variability of diazotroph community composition in the upwelling region off NW Iberia. *Scientific Reports* 2019; **9**: 3737.

20. Moreira-Coello V, Mouriño-Carballido B, Marañón E, Fernández-Carrera A, Bode A, Varela MM. Biological N2 Fixation in the Upwelling Region off NW Iberia: Magnitude, Relevance, and Players. *Frontiers in Marine Science* 2017; **4**.

21. Benavides M, Shoemaker KM, Moisander PH, Niggemann J, Dittmar T, Duhamel S, et al. Aphotic N2 fixation along an oligotrophic to ultraoligotrophic transect in the western tropical South Pacific Ocean. *Biogeosciences* 2018; **15**: 3107–3119.

22. Ward BA, Dutkiewicz S, Moore CM, Follows MJ. Iron, phosphorus, and nitrogen supply ratios define the biogeography of nitrogen fixation. *Limnology and Oceanography* 2013; **58**: 2059–2075.

23. Tang W, Cassar N. Data-Driven Modeling of the Distribution of Diazotrophs in the Global Ocean. *Geophysical Research Letters* 2019; **46**: 12258–12269.

24. Langlois RJ, Mills MM, Ridame C, Croot P, LaRoche J. Diazotrophic bacteria respond to Saharan dust additions. *Mar Ecol Prog Ser* 2012; **470**: 1–14.

25. Mills MM, Turk-Kubo KA, van Dijken GL, Henke BA, Harding K, Wilson ST, et al. Unusual marine cyanobacteria/haptophyte symbiosis relies on N2 fixation even in N-rich environments. *The ISME Journal* 2020; **14**: 2395–2406.

26. Villamaña M, Marañón E, Cermeño P, Estrada M, Fernández-Castro B, Figueiras FG, et al. The role of mixing in controlling resource availability and phytoplankton community composition. *Progress in Oceanography* 2019; **178**: 102181.

27. Cheung S, Nitanai R, Tsurumoto C, Endo H, Nakaoka S, Cheah W, et al. Physical Forcing Controls the Basin-Scale Occurrence of Nitrogen-Fixing Organisms in the North Pacific Ocean. *Global Biogeochemical Cycles* 2020; **34**: e2019GB006452.

28. Arístegui J, Barton ED, Álvarez-Salgado XA, Santos AMP, Figueiras FG, Kifani S, et al. Sub-regional ecosystem variability in the Canary Current upwelling. *Progress in Oceanography* 2009; **83**: 33–48.

29. Castro CG, Pérez FF, Álvarez-Salgado XA, Fraga F. Coupling between the thermohaline, chemical and biological fields during two contrasting upwelling events off the NW Iberian Peninsula. *Continental Shelf Research* 2000; **20**: 189–210.

30. Fraga F. Upwelling off the Galician Coast, Northwest Spain. In: Richards FA (ed). *Coastal Upwelling*. 1981. American Geophysical Union, pp 176–182.

31. Wooster WS, Bakun A, McLain DR. SEASONAL UPWELLING CYCLE ALONG THE EASTERN BOUNDARY OF THE NORTH ATLANTIC. *Journal of Marine Research* 1976; **34**: 131–141.

32. Largier JL. Upwelling Bays: How Coastal Upwelling Controls Circulation, Habitat, and Productivity in Bays. *Annual Review of Marine Science* 2020; **12**: 415–447.

33. Garza-Gil MD, Surís-Regueiro JC, Varela-Lafuente MM. Using input–output methods to assess the effects of fishing and aquaculture on a regional economy: The case of Galicia, Spain. *Marine Policy* 2017; **85**: 48–53.

34. Figueiras FG, Teixeira IG, Froján M, Zúñiga D, Arbones B, Castro CG. Seasonal Variability in the Microbial Plankton Community in a Semienclosed Bay Affected by Upwelling: The Role of a Nutrient Trap. *Front Mar Sci* 2020; **7**.

35. Figueiras FG, Ríos AF. Phytoplankton succession, red tides and the hydrographic regime in the Rias Bajas of Galicia. In: Smayda TJ, Shimizu Y (eds). *Toxic Phytoplankton Blooms in the Sea*. 1993. Elsevier, New York, USA, pp 239–244.

36. Cermeño P, Marañón E, Pérez V, Serret P, Fernández E, Castro CG. Phytoplankton size structure and primary production in a highly dynamic coastal ecosystem (Ría de Vigo, NW-Spain): Seasonal and short-time scale variability. *Estuarine, Coastal and Shelf Science* 2006; **67**: 251–266.

37. Agawin NSR, Benavides M, Busquets A, Ferriol P, Stal LJ, Arístegui J. Dominance of unicellular cyanobacteria in the diazotrophic community in the Atlantic Ocean. *Limnology and Oceanography* 2014; **59**: 623–637.

38. Benavides M, Agawin NSR, Arístegui J, Ferriol P, Stal LJ. Nitrogen fixation by Trichodesmium and small -diazotrophs in the subtropical northeast Atlantic. *Aquat Microb Ecol* 2011; **65**: 43–53.

39. Comesaña A, Fernández-Castro B, Chouciño P, Fernández E, Fuentes-Lema A, Gilcoto M, et al. Mixing and Phytoplankton Growth in an Upwelling System. *Frontiers in Marine Science* 2021; **8**.

40. Broullón E, Franks PJS, Fernández Castro B, Gilcoto M, Fuentes-Lema A, Pérez-Lorenzo M, et al. Rapid phytoplankton response to wind forcing influences productivity in upwelling bays. *Limnology and Oceanography Letters* 2023; **8**: 529–537.

41. Hansen HP, Koroleff F. Determination of nutrients. *Methods of Seawater Analysis*. 1999. pp 159–228.

42. Kérouel R, Aminot A. Fluorometric determination of ammonia in sea and estuarine waters by direct segmented flow analysis. *Marine Chemistry* 1997; **57**: 265–275.

43. Prandke H, Stips A. Test measurements with an operational microstructure-turbulence profiler: Detection limit of dissipation rates. *Aquat Sci* 1998; **60**: 191–209.
44. Deutsch C, Weber T. Nutrient Ratios as a Tracer and Driver of Ocean Biogeochemistry. *Annual Review of Marine Science* . 2012. Annual Reviews. , **4**: 113–141
45. Montoya JP, Voss M, Kahler P, Capone DG. A Simple, High-Precision, High-Sensitivity Tracer Assay for N(inf2) Fixation. *Applied and Environmental Microbiology* 1996; **62**: 986–993.
46. White AE, Granger J, Selden C, Gradoville MR, Potts L, Bourbonnais A, et al. A critical review of the 15N2 tracer method to measure diazotrophic production in pelagic ecosystems. *Limnology and Oceanography: Methods* 2020; **18**: 129–147.
47. Mohr W, Großkopf T, Wallace DWR, LaRoche J. Methodological Underestimation of Oceanic Nitrogen Fixation Rates. *PLOS ONE* 2010; **5**: e12583.
48. Zehr JP, McReynolds LA. Use of degenerate oligonucleotides for amplification of the nifH gene from the marine cyanobacterium Trichodesmium thiebautii. *Applied and Environmental Microbiology* 1989; **55**: 2522–2526.
49. Zehr JP, Turner PJ. Nitrogen fixation: Nitrogenase genes and gene expression. *Methods in Microbiology*. 2001. Academic Press, pp 271–286.
50. Thompson A, Carter BJ, Turk-Kubo K, Malfatti F, Azam F, Zehr JP. Genetic diversity of the unicellular nitrogen-fixing cyanobacteria UCYN-A and its prymnesiophyte host. *Environmental Microbiology* 2014; **16**: 3238–3249.
51. Church MJ, Jenkins BD, Karl DM, Zehr JP. Vertical distributions of nitrogen-fixing phylotypes at Stn Aloha in the oligotrophic North Pacific Ocean. *Aquatic Microbial Ecology* 2005; **38**: 3–14.
52. Moisander PH, Beinart RA, Voss M, Zehr JP. Diversity and abundance of diazotrophic microorganisms in the South China Sea during intermonsoon. *ISME J* 2008; **2**: 954–967.

53. Callahan BJ, McMurdie PJ, Rosen MJ, Han AW, Johnson AJA, Holmes SP. DADA2: High-resolution sample inference from Illumina amplicon data. *Nat Methods* 2016; **13**: 581–583.
54. Angel R, Nepel M, Panhölzl C, Schmidt H, Herbold CW, Eichorst SA, et al. Evaluation of Primers Targeting the Diazotroph Functional Gene and Development of NifMAP – A Bioinformatics Pipeline for Analyzing nifH Amplicon Data. *Front Microbiol* 2018; **9**.
55. Zehr JP, Jenkins BD, Short SM, Steward GF. Nitrogenase gene diversity and microbial community structure: a cross-system comparison. *Environmental Microbiology* 2003; **5**: 539–554.
56. Camacho C, Coulouris G, Avagyan V, Ma N, Papadopoulos J, Bealer K, et al. BLAST+: architecture and applications. *BMC Bioinformatics* 2009; **10**: 421.
57. Heller P, Tripp HJ, Turk-Kubo K, Zehr JP. ARBitrator: a software pipeline for on-demand retrieval of auto-curated nifH sequences from GenBank. *Bioinformatics* 2014; **30**: 2883–2890.
58. Oksanen J, Simpson GL, Blanchet FG, Kindt R, Legendre P, Minchin PR, et al. vegan: Community Ecology Package. 2024.
59. Mouillot D, Stubbs W, Faure M, Dumay O, Tomasini JA, Wilson JB, et al. Niche Overlap Estimates Based on Quantitative Functional Traits: A New Family of Non-Parametric Indices. *Oecologia* 2005; **145**: 345–353.
60. Geange SW, Pledger S, Burns KC, Shima JS. A unified analysis of niche overlap incorporating data of different types. *Methods in Ecology and Evolution* 2011; **2**: 175–184.
61. Martin BD, Witten D, Willis AD. Modeling microbial abundances and dysbiosis with beta-binomial regression. *The Annals of Applied Statistics* 2020; **14**: 94–115.
62. Auladell A, Barberán A, Logares R, Garcés E, Gasol JM, Ferrera I. Seasonal niche differentiation among closely related marine bacteria. *The ISME Journal* 2022; **16**: 178–189.

641 63. Turk-Kubo KA, Mills MM, Arrigo KR, van Dijken G, Henke BA, Stewart B, et al. UCYN-
642 A/haptophyte symbioses dominate N2 fixation in the Southern California Current System.
643 *ISME COMMUN* 2021; **1**: 1–13.
644 64. Zehr JP, Shilova IN, Farnelid HM, Muñoz-Marín M del C, Turk-Kubo KA. Unusual marine
645 unicellular symbiosis with the nitrogen-fixing cyanobacterium UCYN-A. *Nat Microbiol* 2016;
646 **2**: 1–11.
647 65. Selden CR, Mulholland MR, Crider KE, Clayton S, Macías-Tapia A, Bernhardt P, et al. Nitrogen
648 Fixation at the Mid-Atlantic Bight Shelfbreak and Transport of Newly Fixed Nitrogen to the
649 Slope Sea. *Journal of Geophysical Research: Oceans* 2024; **129**: e2023JC020651.
650 66. Shao Z, Xu Y, Wang H, Luo W, Wang L, Huang Y, et al. Global oceanic diazotroph database
651 version 2 and elevated estimate of global oceanic N_2 fixation. *Earth System Science Data*
652 2023; **15**: 3673–3709.
653 67. Harding KJ, Turk-Kubo KA, Mak EWK, Weber PK, Mayali X, Zehr JP. Cell-specific
654 measurements show nitrogen fixation by particle-attached putative non-cyanobacterial
655 diazotrophs in the North Pacific Subtropical Gyre. *Nat Commun* 2022; **13**: 6979.
656 68. Foster RA, Zehr JP. Characterization of diatom–cyanobacteria symbioses on the basis of nifH,
657 hetR and 16S rRNA sequences. *Environmental Microbiology* 2006; **8**: 1913–1925.
658 69. Estrada M. Phytoplankton distribution and composition off the coast of Galicia (northwest of
659 Spain). *Journal of Plankton Research* 1984; **6**: 417–434.
660 70. Ospina-Alvarez N, Varela M, Doval MD, Gómez-Gesteira M, Cervantes-Duarte R, Prego R.
661 Outside the paradigm of upwelling rias in NW Iberian Peninsula: Biogeochemical and
662 phytoplankton patterns of a non-upwelling ria. *Estuarine, Coastal and Shelf Science* 2014;
663 **138**: 1–13.

71. Velasco-Senovilla E, Reguera B, Ramilo I, Casas G, Mouriño-Carballido B, Nogueira E. Upwelling events, depth varying succession of phytoplankton assemblages and vertical connectivity: a conceptual model. *in prep* 2025.

72. Farnelid H, Turk-Kubo K, Muñoz-Marín M del C, Zehr JP. New insights into the ecology of the globally significant uncultured nitrogen-fixing symbiont UCYN-A. *Aquatic Microbial Ecology* 2016; **77**: 125–138.

73. Martínez-García S, Fernández E, Álvarez-Salgado X-A, González J, Lønborg C, Marañón E, et al. Differential responses of phytoplankton and heterotrophic bacteria to organic and inorganic nutrient additions in coastal waters off the NW Iberian Peninsula. *Marine Ecology Progress Series* 2010; **416**: 17–33.

74. Hagino K, Onuma R, Kawachi M, Horiguchi T. Discovery of an Endosymbiotic Nitrogen-Fixing Cyanobacterium UCYN-A in Braarudosphaera bigelowii (Prymnesiophyceae). *PLOS ONE* 2013; **8**: e81749.

75. Cornejo-Castillo FM, Cabello AM, Salazar G, Sánchez-Baracaldo P, Lima-Mendez G, Hingamp P, et al. Cyanobacterial symbionts diverged in the late Cretaceous towards lineage-specific nitrogen fixation factories in single-celled phytoplankton. *Nat Commun* 2016; **7**: 11071.

76. Tripp HJ, Bench SR, Turk KA, Foster RA, Desany BA, Niazi F, et al. Metabolic streamlining in an open-ocean nitrogen-fixing cyanobacterium. *Nature* 2010; **464**: 90–94.

77. Sommer U. The paradox of the plankton: Fluctuations of phosphorus availability maintain diversity of phytoplankton in flow-through cultures. *Limnology and Oceanography* 1984; **29**: 633–636.

78. Teira E, Martínez-García S, Carreira C, Morán X-AG. Changes in bacterioplankton and phytoplankton community composition in response to nutrient additions in coastal waters off the NW Iberian Peninsula. *Marine Ecology Progress Series* 2011; **426**: 87–104.

688 79. Gilcoto M, Largier JL, Barton ED, Piedracoba S, Torres R, Graña R, et al. Rapid response to
689 coastal upwelling in a semienclosed bay. *Geophysical Research Letters* 2017; **44**: 2388–2397.
690 80. Souto C, Gilcoto M, Fariña-Busto L, Pérez FizF. Modeling the residual circulation of a coastal
691 embayment affected by wind-driven upwelling: Circulation of the Ría de Vigo (NW Spain).
692 *Journal of Geophysical Research: Oceans* 2003; **108**.
693 81. Álvarez-salgado XA, Castro CG, Pérez FF, Fraga F. Nutrient mineralization patterns in shelf
694 waters of the Western Iberian upwelling. *Continental Shelf Research* 1997; **17**: 1247–1270.
695 82. Rosón G, Álvarez-Salgado XA, Pérez FF. Carbon cycling in a large coastal embayment,
696 affected by wind-driven upwelling: short-time-scale variability and spatial differences.
697 *Marine Ecology Progress Series* 1999; **176**: 215–230.
698 83. Garber JH. Laboratory study of nitrogen and phosphorus remineralization during the
699 decomposition of coastal plankton and seston. *Estuarine, Coastal and Shelf Science* 1984; **18**:
700 685–702.
701 84. Nogueira E, Pérez FF, Ríos AF. Seasonal Patterns and Long-term Trends in an Estuarine
702 Upwelling Ecosystem (Ría de Vigo, NW Spain). *Estuarine, Coastal and Shelf Science* 1997; **44**:
703 285–300.
704 85. Pérez FF, Álvarez-Salgado XA, Rosón G. Stoichiometry of the net ecosystem metabolism in a
705 coastal inlet affected by upwelling. The Ría de Arousa (NW Spain). *Marine Chemistry* 2000;
706 **69**: 217–236.
707 86. Alonso-Pérez F, Castro CG. Benthic oxygen and nutrient fluxes in a coastal upwelling system
708 (Ria de Vigo, NW Iberian Peninsula): seasonal trends and regulating factors. *Marine Ecology*
709 *Progress Series* 2014; **511**: 17–32.
710 87. Padin XA, Velo A, Pérez FF. ARIOS: a database for ocean acidification assessment in the
711 Iberian upwelling system (1976–2018). *Earth System Science Data* 2020; **12**: 2647–2663.

712 88. Álvarez-Salgado XA, Borges A, Figueiras FG, Chou L. Iberian margin: the Rías. *Carbon and*
713 *Nutrient Fluxes in Continental Margins* 2010; 102–119.
714 89. Marañón E, Cermeño P, Huete-Ortega M, López-Sandoval DC, Mouriño-Carballido B,
715 Rodríguez-Ramos T. Resource Supply Overrides Temperature as a Controlling Factor of
716 Marine Phytoplankton Growth. *PLOS ONE* 2014; **9**: e99312.
717 90. Singh A, Bach LT, Fischer T, Hauss H, Kiko R, Paul AJ, et al. Niche construction by non-
718 diazotrophs for N2 fixers in the eastern tropical North Atlantic Ocean. *Geophysical Research*
719 *Letters* 2017; **44**: 6904–6913.
720

Figure legends

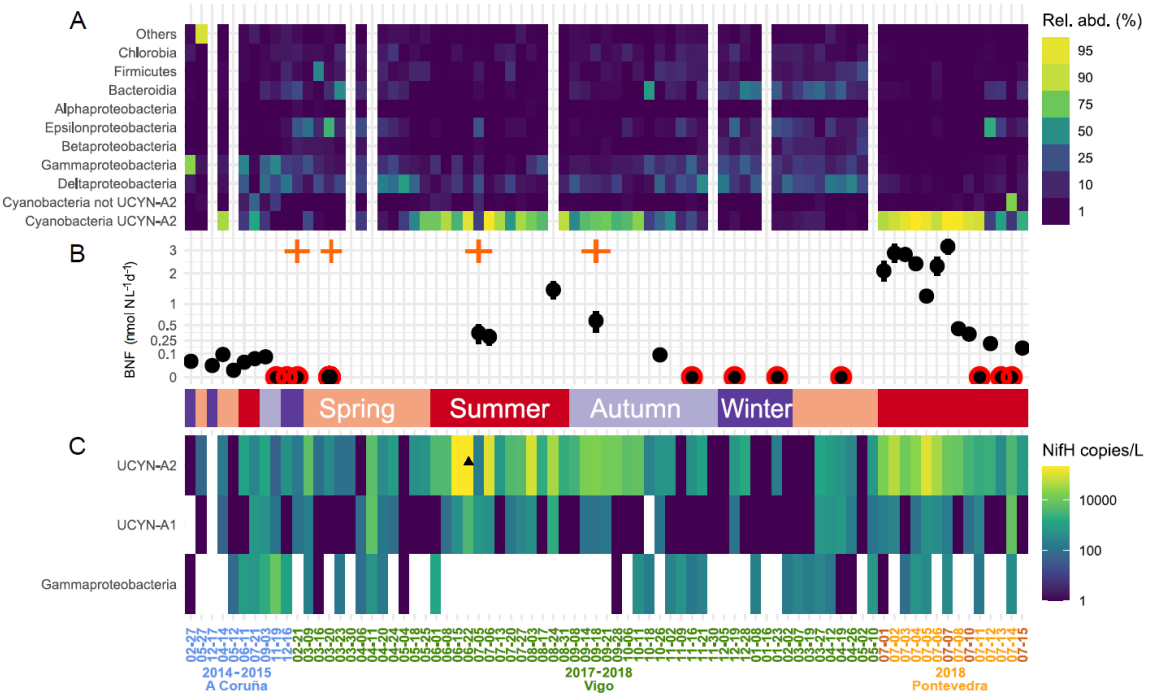

Figure 1. Diazotrophic abundance and community composition, and biological nitrogen fixation. Temporal variability of **A)** *nifH* amplicon-based sequencing community composition (relative abundance %) for the most abundant taxa, ordered from top to bottom in increasing abundance. Blank gaps are discarded samples due DNA extraction issues or unacceptable rarefaction curves. **B)** Nitrogen fixation rate (nmol N $L^{-1}d^{-1}$) measurements. When values were below detection limits, they are represented with a red border. Error bars represents triplicate measurements (if not visible, they are not larger than the dots). Note the square root transformation on the y-axis (not linear to help in the visualization of small values). **C)** quantitative *nifH* gene copy abundance (qPCR, *nifH* gene copies L^{-1}) data for UCYN-A2, UCYN-A1 and *Gammaproteobacteria* 24774A11. Note that the color scale is logarithmic. UCYN-A2 abundance on 22nd June 2017 exceeded the scale's range by an order of magnitude ($1.7 \pm 0.7 \times 10^6$ *nifH* transcripts copies·L^{-1}), and it was replaced by a black triangle for visualization purposes. The same figure without this visual solution can be seen

736 in Fig. S9. Climatological season is represented in the inner colored band. The x-axis is
737 shared for the three graphs, sampling dates (format: year/month/day) colored according to
738 location (color code for the locations in Fig. S1). Times when nitrogen amendment
739 experiments were performed are indicated with orange crosses in the upper margin of B).

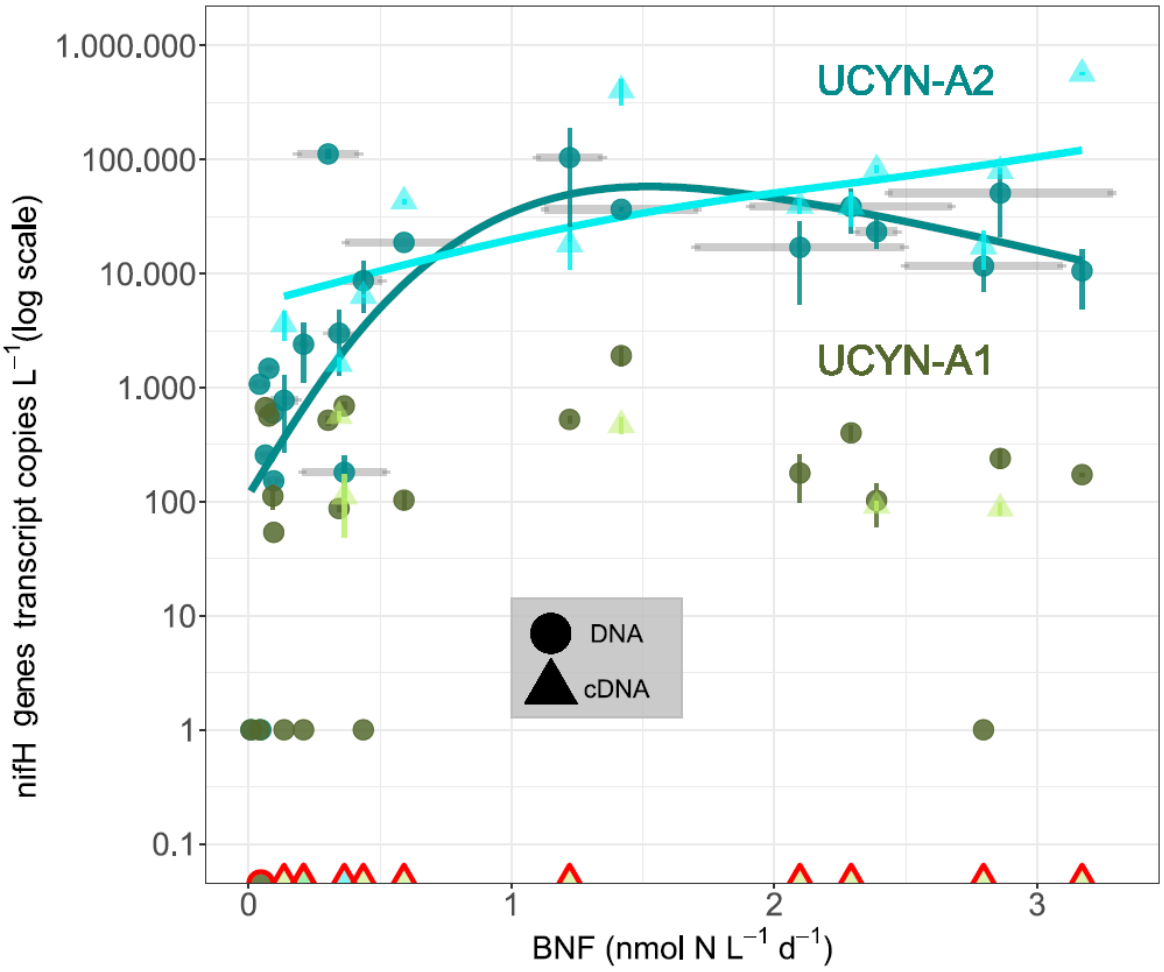

740

741 **Figure 2. UCYN-A *nifH* gene abundance and expression.** Relationship between BNF
742 (nmol N $L^{-1}d^{-1}$) and the abundance of UCYN-A ecotypes (A1 and A2). Quantification of *nifH*
743 gene copies/L by qPCR from DNA (circles) and *nifH* gene transcripts/L by RT-qPCR from
744 cDNA (triangles). Note that the y-scale is logarithmic. Error bars in the y-axis represent
745 standard deviation from three replicates per sample (if not visible, they are not larger than
746 the dots). Uncertainty in N_2-fixation rates is represented in the x-axis with gray horizontal

bars spanning the triplicates measurements (only for UCYN-A2). Samples with positive BNF and non-detection by qPCR are included on the x-axis with red bordering.

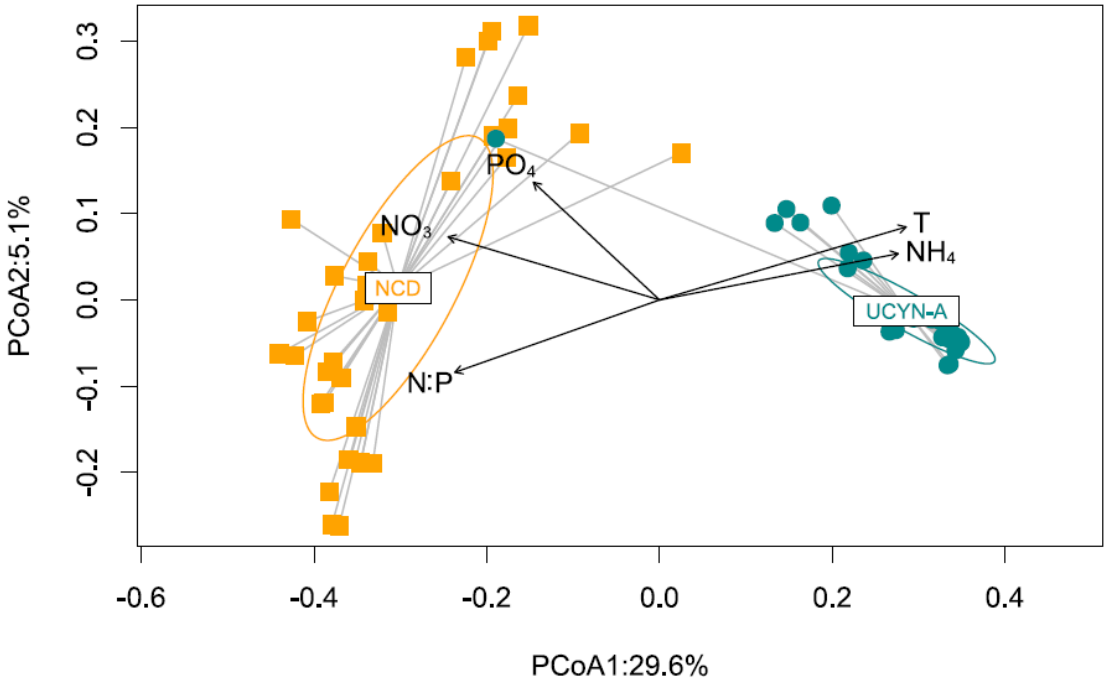

Figure 3. Taxa dominance is related with environmental conditions. Principal Coordinates Analysis (PCoA) based on Bray-Curtis dissimilarity matrix illustrating the differences between samples dominated by UCYN-A (cyan circles) and non-cyanobacterial diazotrophs (NCD, orange squares). Sample group centroids for each dominance situation and confidence ellipses displaying the standard deviation of centroid locations are also represented. The environmental factors (%NH_4^+, N:P ratio, in situ temperature, NO_3^- and PO_4^{3-}) that contributed most to the community differences observed between these dominance situations were fitted through significant ($p < 0.001$) vector overlays (black color) onto the PCoA ordination. The first axis of the PCoA (x-axis) explains 29.4% of the variance, and the second axis (y-axis) 5.1%.

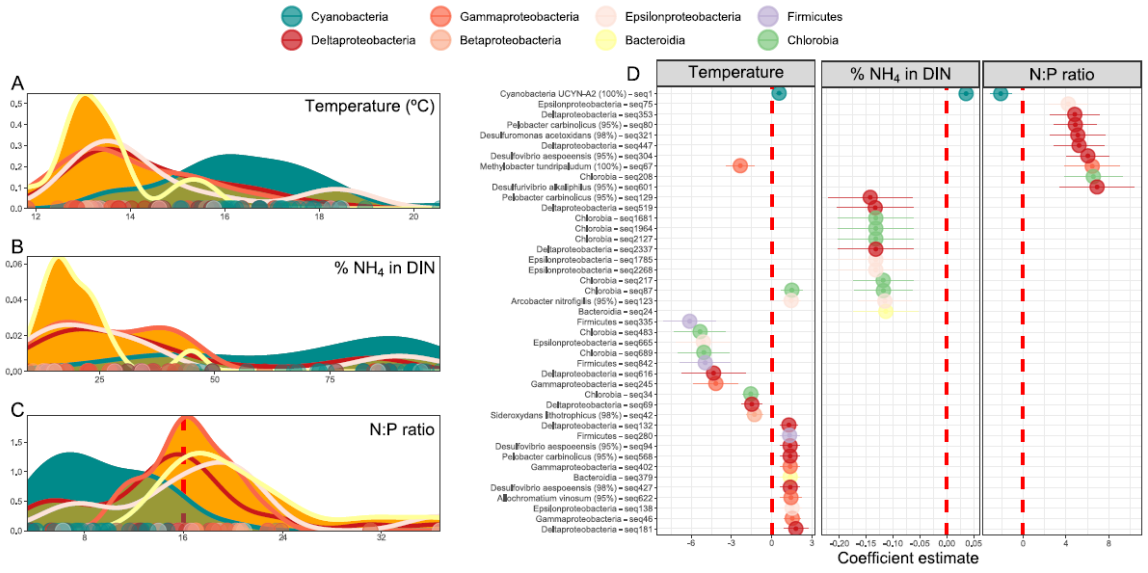

Figure 4. Temperature and inorganic nitrogen conditions are niche descriptors of the diazotrophic community. A) Kernel density estimates for the taxonomical groups and the niche descriptors temperature (ºC, A) and inorganic nutrient content, (% of NH_4^+ in total DIN, B; N:P ratio, B;) and separated by cyanobacterial (cyan) and non-cyanobacterial diazotrophs (orange). The red vertical line in C) at N:P ratio=16 delimits apparent nitrogen limitation conditions (when the ratio is <16, left side of the graph). Deviations from N:P ratio=16 (red dashed line in Fig. 4C) separate conditions when there is phosphorus in excess (on the left side of the plot) from conditions of nitrogen surplus (on the right side). The y-axis represents the probability density function for the kernel density estimation. B) Coefficients of models after beta-binomial regression for the environmental parameters temperature (right column) and inorganic nutrient content (% of NH_4^+ in total DIN, mid; N:P ratio, left column). Only significant models ($p \leq 0.05$) from the whole diazotroph community (7030 ASVs) are shown. The coefficient estimate indicates positive or negative responses to the parameter and is shown with a 95% confidence interval. Specie identification in the y-axis label is only shown when BLASTp result is >=95% (percentage in parentheses). A detailed table with taxonomy

info and complete *nifH* sequence for each one of these ASVs is available in the Table S7. The color code is shared at taxa level for both panels.

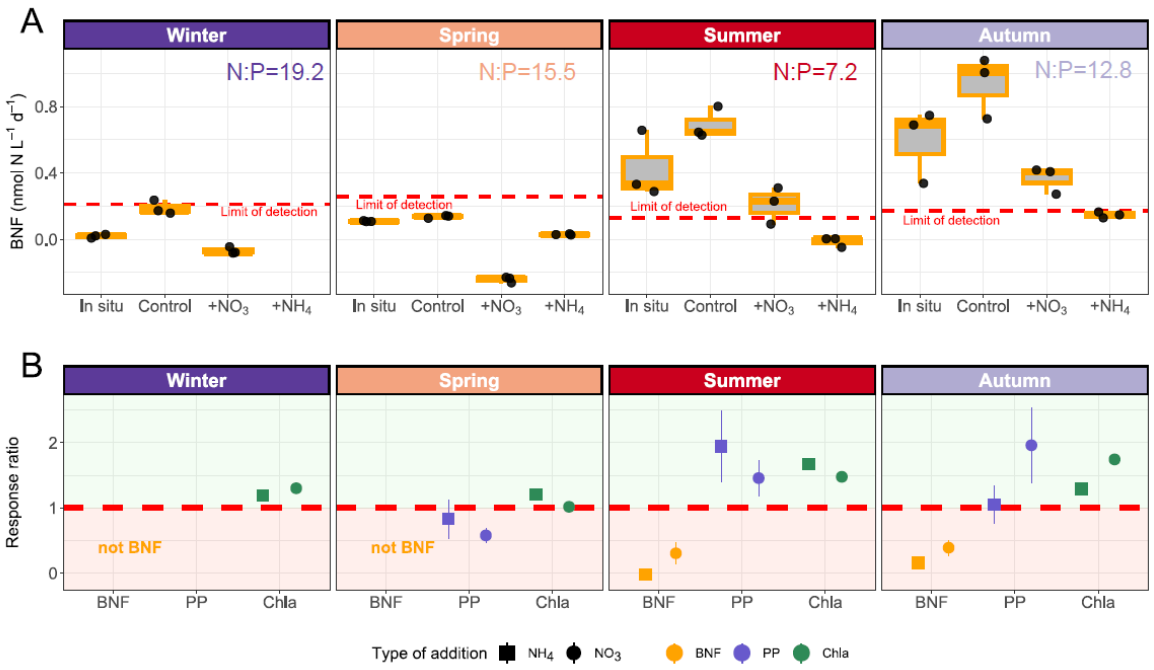

Figure 5. Biological nitrogen fixation (BNF) decreases with inorganic nitrogen additions when the plankton community is N-limited. Response of BNF, primary production rates and C*hl a* after nutrient amendment microcosm experiments through each climatological season (n= 4) **A)** BNF (nmol N $L^{-1}d^{-1}$) at in situ conditions (natural environment), inside the microcosm setting ("*Control*") and the response after 24 hours in the nitrate ($+NO_3^-$) or ammonia ($+NH_4^+$) amendment treatments. Red dashed horizontal line represents the methodological limit of detection for each triplicate of measurements (black dots). **B)** Response ratio defined as the change in absolute value of the variable with regard to control conditions after 24 hours. Values below 1 (red dashed line) are mean reductions and values above 1 mean increases.

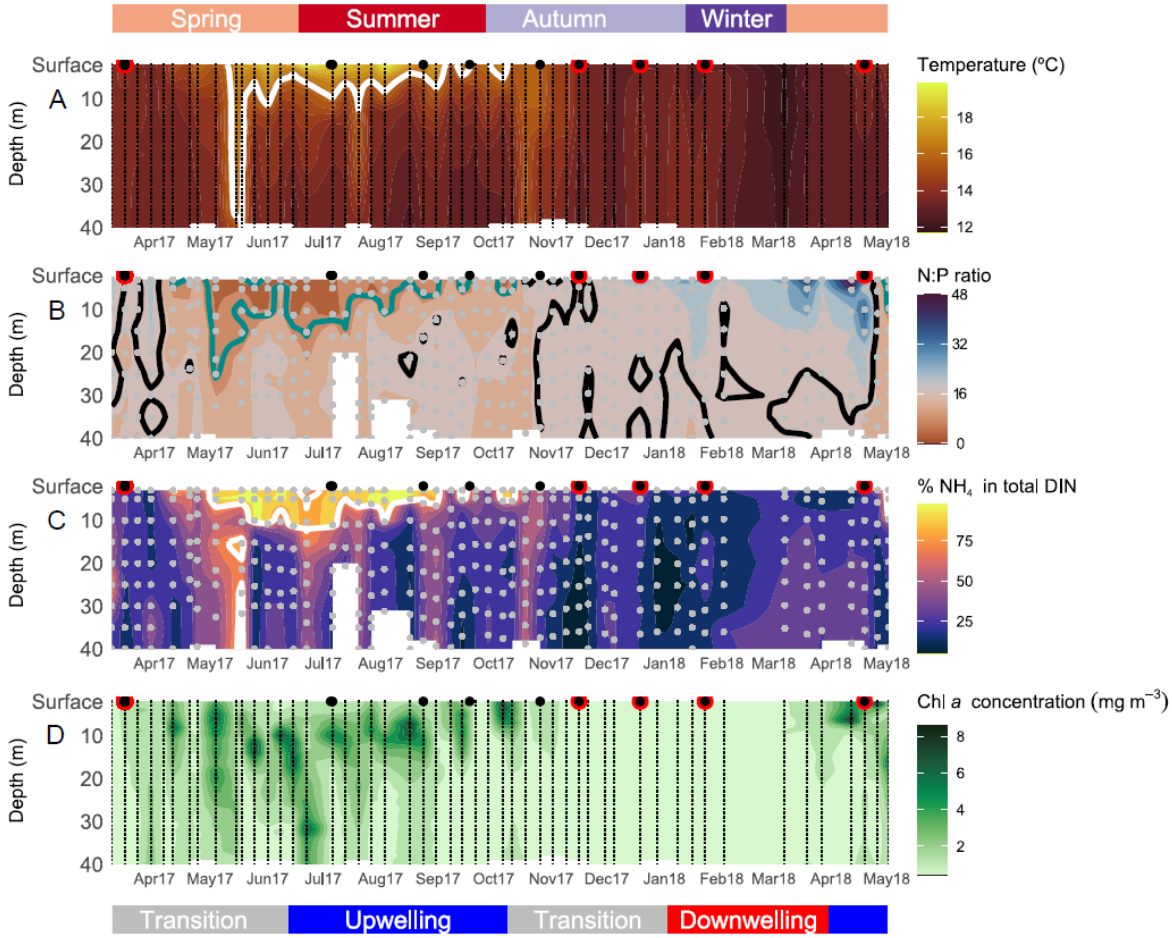

790

791 **Figure 6. Hydrographic full-depth variability at weekly resolution at the central Ria de**
792 **Vigo during spring 2017 – spring 2018.** Time-series of the full-depth vertical distribution
793 of A) temperature (ºC). The white solid line represents the isotherm of 16 ºC. B) N:P ratio.
794 The green and black solid line represents the isoline of 7.2 and 16, respectively. C) % of
795 NH_4^+ in DIN. The white solid line represents the isoline of 75%. And D) Chlorophyll *a* (Chl *a*)
796 concentration ($mg \cdot m^{-3}$). Dots represent sample vertical resolution. Surface black circles
797 represents nitrogen fixation rate measurements. When values were below detection limits,
798 they are represented with a red border. Climatological season is represented in the top
799 colored band. The hydrographic conditions with respect to upwelling (blue), downwelling
800 (red), and transition (gray) in the low colored band following[39].

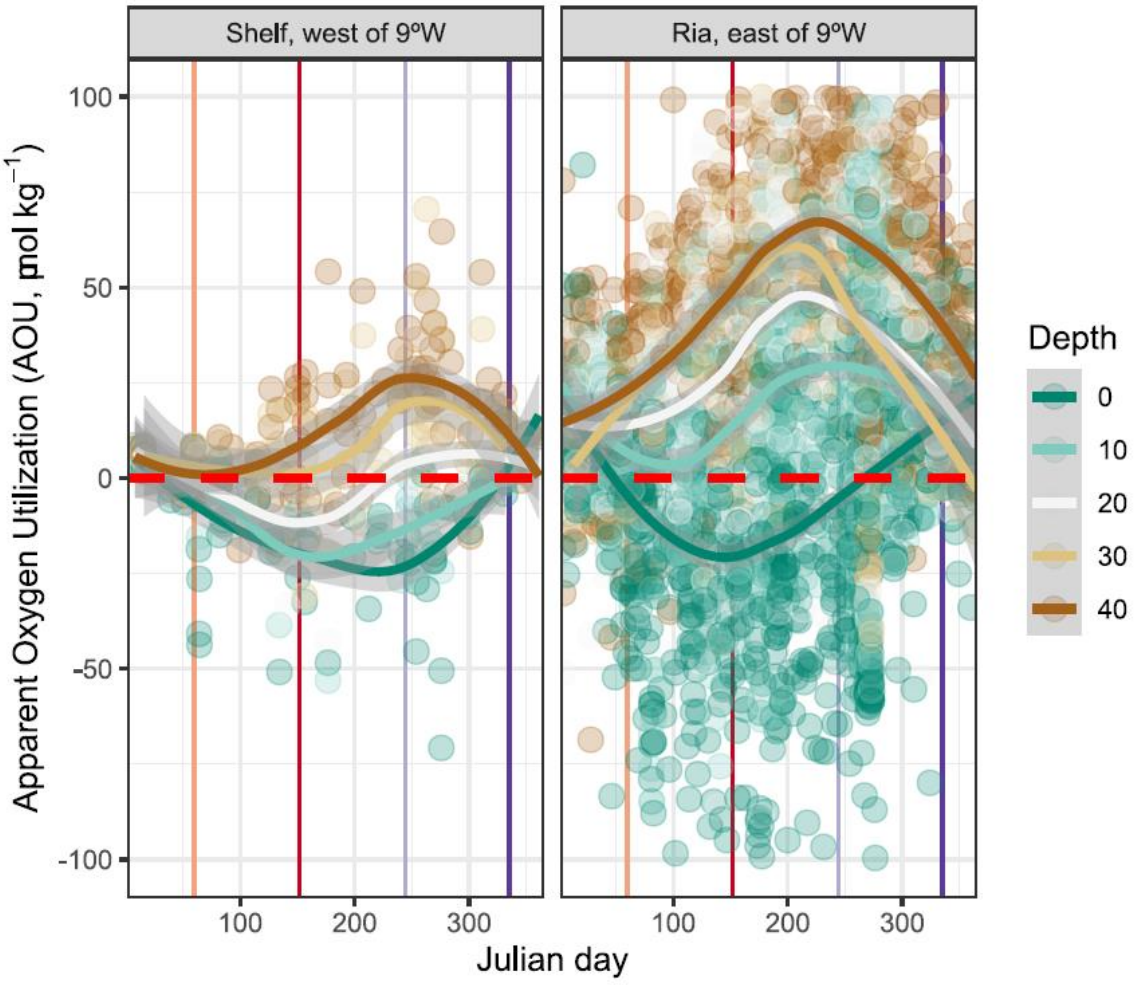

Figure 7. Annual variability of apparent oxygen utilization (AOU, µmol kg^{-1}), a proxy of the biological production and consumption of oxygen, at the Ria de Vigo. It includes discrete samples of measured dissolved oxygen data from 1986-2018[87] and the shelf/Ría separation criteria (panels left and right) was considered at 9ºW longitude (westernmost location 9.5ºW). Depth bands grouped each 10 m, from surface (0 m) to bottom (40 m, maximum depth of central Ria de Vigo station) have been modelled with a locally weighted polynomial regression (LOESS). Oversaturation of oxygen due biological production (AOU

<0, μmol kg^{-1}) and undersaturation due respiration (AOU>0, μmol kg^{-1}) are separated by the red-dashed line. The vertical solid lines represent the onset of climatological seasons.

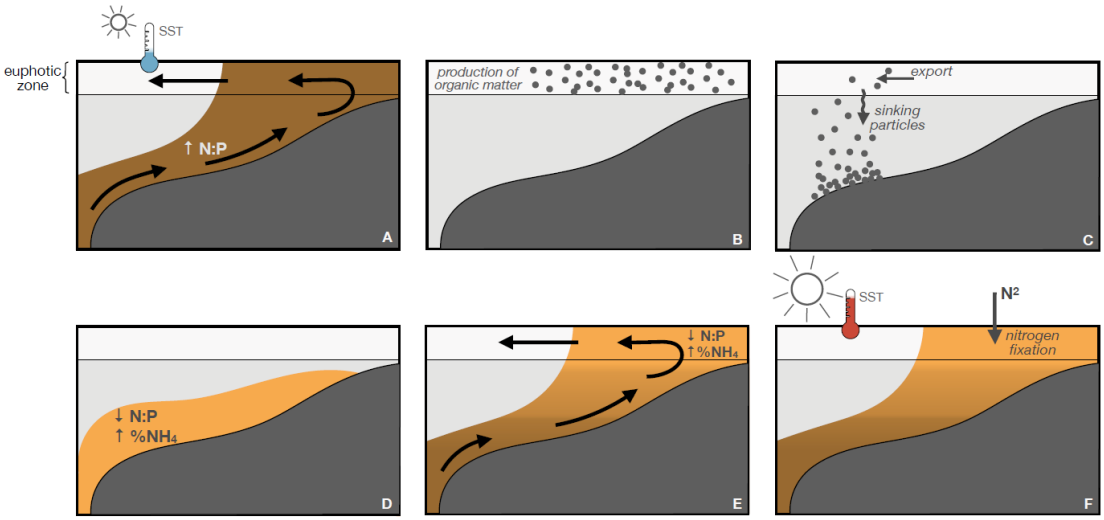

Figure 8. The sequential steps of the mechanistic biogeochemical niche construction process for nitrogen fixers. (A) At the beginning of the upwelling season, sea surface temperature (SST) is still cold. Upwelled ENACW brings nutrients upwards, into the ría, sustaining an elevated N:P ratio and low content in the form of NH_4^+. (B) Phytoplankton grow within the surface layer due to the previous nutrient input and the necessary irradiance. Subsequently, (C) organic matter produced by phytoplankton is exported to the outer part of the ría, where it sinks. (D) This organic matter is remineralized near the bottom, where P content rapidly increases, lowering N:P levels. There, inorganic nitrogen is mostly in the form of NH_4^+. (E) Further into the upwelling season, upwelled waters are mixed with the remineralized P-rich waters, and positive upwelling circulation transports them towards the surface. (F) At the end of the summer upwelling season, SST has increased (> 16 ºC) and nitrogen fixers can take an advantage of it, in combination to the low N:P conditions.

Acknowledgements

MF was funded by Juan de La Cierva Formación (FJC2019-038970-I, Ministerio de Ciencia e Innovación, Spanish Government). Additional funds for molecular analysis were coming from Axencia Galega de Innovacion (agreement GAIN-IEO) and GRC-EPB Plankton Ecology and Biogeochemistry Research Group (ref. IN607A2018/2). This research was funded by project REMEDIOS (CTM2016-75451-C2-1-R) to BM-C from the Spanish Ministry of Economy and Competitiveness. Bioinformatic analysis were partially run at the Centro de Supercomputación de Galicia (CESGA). AFC was supported by Xunta de Galicia 2013 postdoctoral fellowship POS-A/2013/142 and Beatriz Galindo fellowship BG22-00067. We thank E. Teira, E. Fernández, A. Fuentes, M. Pérez, E. Peláez and S. Vieitez, M. J. Pazó, V. Vieitez, C. Rodríguez, J. Valencia, R. Alba-Salgueiro for their assistance during field experiments and lab analysis. We thank X. A. Álvarez-Salgado for his helpful comments on an early version of the draft. Th authors thank the Editor-in-Chief, Janet E. Hill, and two anonymous reviewers for their constructive and helpful comments.

Data Availability Statement

Source datasets supporting the current study are available in https://figshare.com/collections/Mixing_and_Phytoplankton_Growth_in_an_Upwelling_System/5604209 and https://data.mendeley.com/datasets/pm4r2pyyh3/2. *nifH* sequences are deposited in SRA with accession number PRJNA1184991 https://www.ncbi.nlm.nih.gov/bioproject/PRJNA1184991. Code and data to reproduce the results is publicly available in https://github.com/mfontela/nifH_niche